
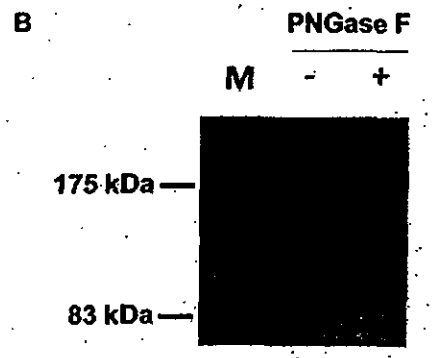


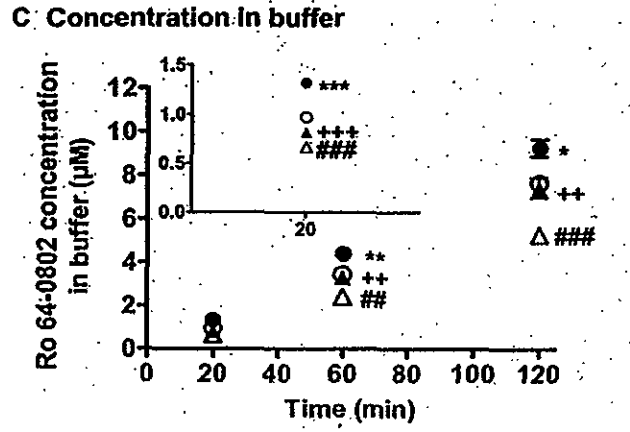


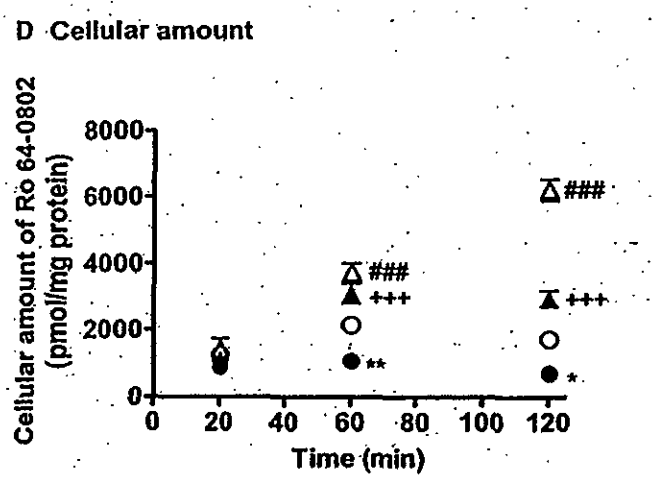


FIG. 1. Efflux of intracellularly formed Ro 64-0802 from mock-transfected and MRP4-expressing MDCKII cells. A and B, Western blotting. A, cell lysates were prepared from mock-transfected (GFP/CES1A1-MDCKII) and MRP4-expressing MDCKII cells (MRP4/CES1A1-MDCKII) and subjected to SDS-polyacrylamide gel electrophoresis (7.5%). B, *N*-linked carbohydrate groups were cleaved from the MRP4 protein in the cell lysates using *N*-glycosidase F (PNGase F). MRP4 was detected by the monoclonal anti-MRP4 M4I-10 antibody. C and D, efflux transport study: MRP4/CES1A1-MDCKII (●, ▲) and GFP/CES1A1-MDCKII cells (○, △) were incubated with 10 μM oseltamivir in the presence (▲, △) or absence (●, ○) of indomethacin (50 μM) at 37°C. Each point represents the mean ± S.E. ($n = 6$). Statistical significance was calculated by one-way ANOVA followed by Tukey's multiple comparison test. *, $P < 0.05$; **, $P < 0.01$; ***, $P < 0.001$; significantly different between MRP4/CES1A1-MDCKII and GFP/CES1A1-MDCKII cells. ##, $P < 0.01$; ###, $P < 0.001$; significantly different in GFP/CES1A1-MDCKII cells with and without indomethacin. ++, $P < 0.01$; +++, $P < 0.001$; significantly different in MRP4/CES1A1-MDCKII cells with and without indomethacin.

mice exhibited delayed elimination of Ro 64-0802 from the brain compared with that in wild-type mice.

**Efflux of Ro 64-0802 from the Cerebral Cortex of Wild-Type and *Mrp4*$^{-/-}$ Mice after Microinjection.** Real-time PCR was used to check the adaptive regulation of efflux transporters at the BBB of *Mrp4*$^{-/-}$ mice. No significant differences were observed in the mRNA expression levels of Mdr1a, Bcrp, Oat3, Oatp1a4, or Oatp1c1 in the cerebral cortex, quantified by real-time PCR, between wild-type and *Mrp4*$^{-/-}$ mice (data not shown).

To examine the involvement of Mrp4 in the efflux transport of Ro 64-0802 across the BBB, Ro 64-0802 was directly injected into the mouse cerebral cortex, and the amount of Ro 64-0802 remaining in the brain was determined at 60 and 120 min after injection. The amount of Ro 64-0802 remaining in the brain was compared between wild-type and *Mrp4*$^{-/-}$ mice (Fig. 4). As shown in Fig. 4, *Mrp4*$^{-/-}$ mice exhibited delayed elimination of Ro 64-0802 from the brain compared with that in wild-type mice.

**Brain/Plasma Concentration Ratio of Ro 64-0802 after Subcutaneous Infusion of Oseltamivir or Ro 64-0802 in Wild-Type, *Oat3*$^{-/-}$, and *Mrp4*$^{-/-}$ Mice.** To clarify the importance of the Oat3- and Mrp4-mediated efflux of Ro 64-0802 at the BBB, Ro 64-0802 was given to mice by subcutaneous infusion for 24 h, and the $K_{p,brain}$ of Ro 64-0802 was determined. The concentrations of Ro 64-0802 in

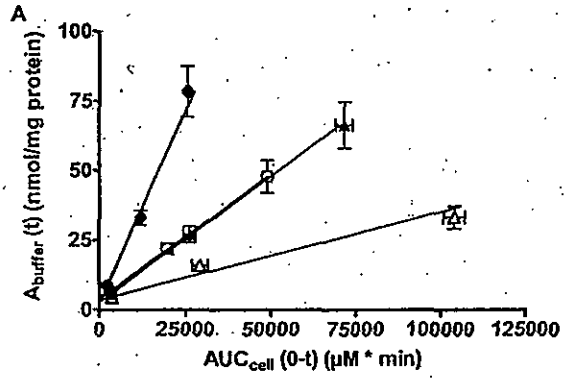


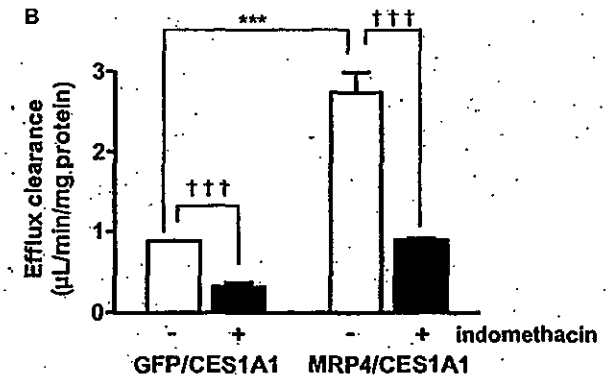


FIG. 2. Integration plots of the efflux transport of Ro 64-0802 from MRP4/CES1A1-MDCKII and GFP/CES1A1-MDCKII cells. A, integration plot: the amount of Ro 64-0802 in buffer [$A_{buffer}$ ($t$)] was plotted against $AUC_{cell}$ (0–$t$) in MRP4/CES1A1-MDCKII (●, ▲) and GFP/CES1A1-MDCKII cells (○, △) in the presence (▲, △) or absence (●, ○) of indomethacin (50 μM). The data used for the calculation are cited in Fig. 1, C and D. The slope of the plot represents the efflux clearance. Each point represents a mean ± S.E. ($n = 6$). B, efflux clearance of Ro 64-0802: The efflux clearance of Ro 64-0802 was calculated from the slope of the integration plot (A). Statistical significance was calculated by one-way ANOVA followed by Tukey's multiple comparison test. ***, $P < 0.001$; significantly different between MRP4/CES1A1-MDCKII and GFP/CES1A1-MDCKII cells. †††, $P < 0.001$; significantly different efflux clearance in the presence and absence of indomethacin. Data represent means ± computer-calculated S.D. (microliters per minute per milligram of protein).

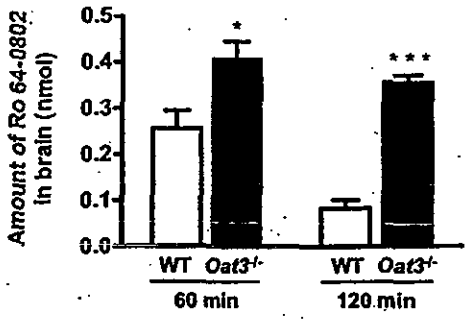


FIG. 3. Comparison of the amounts of Ro 64-0802 in the ipsilateral cerebrum after intracerebral microinjection of Ro 64-0802 in wild-type (WT) and *Oat3*$^{-/-}$ mice. *Ro 64-0802 (1 mM) in 0.5 μl of ECF buffer was injected into the Par2 region (4.5* mm lateral to the bregma and 2.5 mm in depth). The amount of Ro 64-0802 in the ipsilateral cerebrum was determined at 60 and 120 min after treatment. □, data for wild-type mice; ■, data for *Oat3*$^{-/-}$ mice. Each bar represents the mean ± S.E. *(n = 3–4). Statistically significant differences between wild-type and Oat3*$^{-/-}$ mice: *, $P < 0.05$; ***, $P < 0.001$.

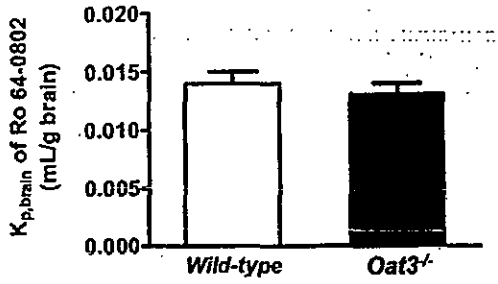


FIG. 5. Comparison of the brain/plasma concentration ratio ($K_{p,brain}$) of Ro 64-0802 after subcutaneous infusion of Ro 64-0802 in wild-type and *Oat3*$^{-/-}$ mice. Mice received a continuous subcutaneous infusion of Ro 64-0802 at a dose of 80 nmol/h/mouse for 24 h, with an osmotic pump. The plasma and brain concentrations of Ro 64-0802 were determined at 24 h after treatment. □, data for wild-type mice; ■, data for *Oat3*$^{-/-}$ mice. Each bar represents the mean ± S.E. ($n$ = 3–4).

the plasma were 4.5 ± 0.6 and 4.5 ± 1.3 μM in wild-type and *Oat3*$^{-/-}$ mice, respectively. The $K_{p,brain}$ of Ro 64-0802 in *Oat3*$^{-/-}$ mice was not significantly different from that in wild-type mice and remained close to the capillary volume in the brain (Fig. 5). After subcutaneous infusions of oseltamivir in wild-type or *Mrp4*$^{-/-}$ mice, the plasma concentrations of Ro 64-0802 were 6.9 ± 2.3 and 12 ± 5 μM, respectively. The $K_{p,brain}$ of Ro 64-0802 was 3.8-fold higher in *Mrp4*$^{-/-}$ mice than that in wild-type mice (Fig. 6). Even after subcutaneous infusions of Ro 64-0802, the $K_{p,brain}$ of Ro 64-0802 was 6.4-fold greater in *Mrp4*$^{-/-}$ mice than that in wild-type mice (Fig. 6). The plasma concentrations of Ro 64-0802 were 5.7 ± 0.8 and 3.8 ± 1.7 μM in wild-type and *Mrp4*$^{-/-}$ mice treated with Ro 64-0802, respectively.

## Discussion

Abnormal behavior is a suspected adverse effect of oseltamivir on the central nervous system. To understand the pharmacological action of oseltamivir in the brain, its uptake and efflux transport across the BBB were investigated as factors that determine its exposure to the central nervous system. In this study, we focused on Oat3 and Mrp4 as transporters of Ro 64-0802, a pharmacologically active form of oseltamivir, across the BBB.

First, we examined the involvement of Oat3 in the elimination of Ro 64-0802 from the cerebral cortex after microinjection because an in vitro transport study using OAT3-expressing HEK cells identified Ro 64-0802 as a substrate of OAT3. The elimination of Ro 64-0802 from the brain after its microinjection into the cerebral cortex was markedly delayed in *Oat3*$^{-/-}$ mice compared with wild-type mice (Fig. 3). This suggests that Oat3 plays a significant role in the efflux of Ro 64-0802 from the brain by facilitating its uptake from the brain interstitial space to endothelial cells. For the directional efflux of Ro 64-0802 from the brain to the blood across the BBB, a transporter(s) is also required to facilitate its luminal efflux, considering the hydrophilic nature of Ro 64-0802. In a previous study, we demonstrated that the brain concentrations of Ro 64-0802 in *Mdr1a/1b*$^{-/-}$ and *Abcg2*$^{-/-}$ mice are similar to that in wild-type mice (Ose et al., 2008), excluding the possibility that P-gp and Bcrp are involved in the luminal efflux of Ro 64-0802. Therefore, we focused on Mrp4, another ATP-binding cassette transporter at the BBB, as a candidate transporter because it has been reported to mediate the active efflux of topotecan and adefovir across the BBB (Leggas et al., 2004; Belinsky et al., 2007). To show that Ro 64-0802 is a substrate of MRP4, we constructed double transfectant cells expressing both CES1A1, an enzyme producing Ro 64-0802 from oseltamivir, and MRP4 (MRP4/CES1A1-MDCKII). The double transfectant exhibited enhanced efflux of Ro 64-0802 (which was inhibited by an MPR4 inhibitor, indomethacin) compared with GFP/CES1A1-MDCKII (Fig. 2B). It should be noted that the host cells also exhibited indomethacin-sensitive efflux of Ro 64-0802. This is presumably attributable to endogenous canine MRP4 because its mRNA expression was detected by reverse transcription-PCR in MDCKII cells (data not shown). The involvement of Mrp4 in the efflux of Ro 64-0802 across the BBB was

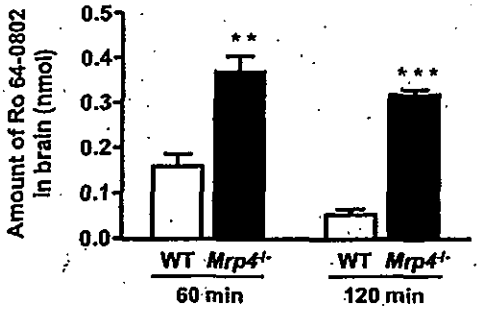


FIG. 4. Comparison of the amounts of Ro 64-0802 in the ipsilateral cerebrum after intracerebral microinjection of Ro 64-0802 in wild-type (WT) and *Mrp4*$^{-/-}$ mice. *Ro 64-0802 (1 mM) in 0.5 μl of ECF buffer was injected into the Par2 region (4.5* mm lateral to the bregma and 2.5 mm in depth). The amount of Ro 64-0802 in the ipsilateral cerebrum was determined at 60 and 120 min after treatment. □, data for wild-type mice; ■, data for *Mrp4*$^{-/-}$ mice. Each bar represents the mean ± S.E. *(n = 3–4). Statistically significant differences between wild-type and Mrp4*$^{-/-}$ mice: **, $P < 0.01$; ***, $P < 0.001$.

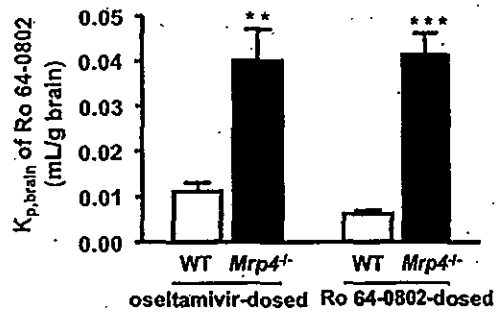


FIG. 6. Comparison of the brain/plasma concentration ratio ($K_{p,brain}$) of Ro 64-0802 after subcutaneous infusion of either oseltamivir or Ro 64-0802 in wild-type (WT) and *Mrp4*$^{-/-}$ mice. Mice received a continuous subcutaneous infusion of either *oseltamivir or Ro 64-0802 at a dose of 400 or 80 nmol/h/mouse, respectively, for* 24 h with an osmotic pump. The plasma and brain concentrations of Ro 64-0802 were determined at 24 h after treatment. □, data for wild-type mice; ■, data for *Mrp4*$^{-/-}$ mice. Each bar represents the mean ± S.E. ($n$ = 4–6). Statistically *significant differences between wild-type and Mrp4*$^{-/-}$ mice: **, $P < 0.01$; ***, $P < 0.001$.

then examined using *Mrp4*$^{-/-}$ mice by microinjection into the cerebral cortex. *Mrp4*$^{-/-}$ mice exhibited delayed elimination of Ro 64-0802 from the cerebral cortex after its microinjection compared with that in wild-type mice (Fig. 4). Therefore, Mrp4 plays an important role in the luminal efflux of Ro 64-0802 after its cellular uptake by Oat3 from the brain side.

To show the importance of the active efflux of Ro 64-0802 at the BBB mediated by Oat3 and Mrp4, the $K_{p,\,brain}$ of Ro 64-0802 was determined in *Oat3*$^{-/-}$ or *Mrp4*$^{-/-}$ mice given Ro 64-0802 by subcutaneous infusion for 24 h. Our approach was based on the pharmacokinetic concept that reduced efflux across the BBB may lead to an increase in the $K_{p,\,brain}$. Consistent with a previous report (Ose et al., 2008), the $K_{p,\,brain}$ of Ro 64-0802 was close to the capillary volume in wild-type mice. The $K_{p,\,brain}$ of Ro 64-0802 observed in *Oat3*$^{-/-}$ mice was also close to the capillary volume (Fig. 5). In contrast, the $K_{p,\,brain}$ of Ro 64-0802 was 4- to 6-fold greater in *Mrp4*$^{-/-}$ mice than that in wild-type mice receiving either oseltamivir or Ro 64-0802 (Fig. 6). These in vivo results using *Mrp4*$^{-/-}$ mice thus indicate that Ro 64-0802 crosses the BBB from the blood side to the brain, but Mrp4 limits its penetration into the brain by extruding it into the blood. The latter finding is consistent with the results of our microinjection experiment. However, the lack of effect of knockout of *Oat3* on the $K_{p,\,brain}$ of Ro 64-0802 seems to contradict the results of the microinjection experiment. There are three explanations for this discrepancy. The first explanation is that luminal Mrp4 is more important in preventing brain penetration than abluminal Oat3. The second explanation is that, considering the mediation of bidirectional transport by Oat3 (Bakhiya et al., 2003), it is possible that Oat3 on the abluminal membrane of brain endothelial cells may act in the efflux of Ro 64-0802 from inside the endothelial cells into the brain, as well as in its uptake from the brain to the endothelial cells (Fig. 7). The third explanation is that, considering the hydrophilic character of Ro 64-0802, with an anionic charge, its luminal uptake probably involves transporters. Kikuchi et al. (2003) suggested that Oat3 is expressed on both the luminal and abluminal membranes of rat brain capillaries; however, this localization is controversial (Mori et al., 2003; Roberts et al., 2008). Oat3 may serve as an uptake system for Ro 64-0802 on the luminal membrane from the circulating blood into the brain (Fig. 7). Further studies using *Mrp4* and *Oat3* double knockout mice can answer these questions and perhaps confirm these speculations.

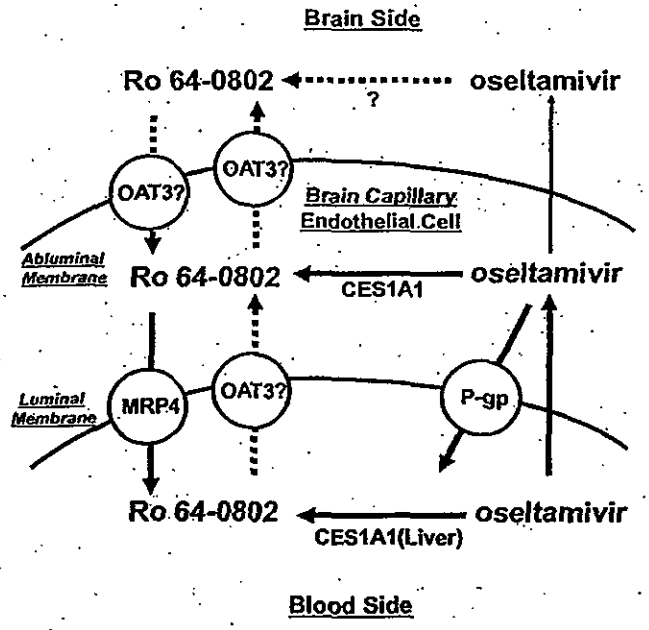


FIG. 7. Schematic representation of the proposed mechanism underlying the brain distribution of oseltamivir and Ro 64-0802 in humans. Oseltamivir crosses the BBB, and Ro 64-0802 is produced by CES1A1 during the penetration of oseltamivir across the BBB. Both oseltamivir and Ro 64-0802 are subjected to active efflux by P-gp and MRP4, respectively. The functional importance of OAT3 at the human BBB has not yet been established, so the hypothetical pathway is shown with a broken line.

Figure 7 summarizes the proposed mechanisms determining the brain distribution of oseltamivir and Ro 64-0802 in humans. P-gp, MRP4, and CES1A1 are factors that determine the brain distribution of oseltamivir and Ro 64-0802 in humans. CES1A1 is predominantly expressed in the brain capillaries in human brain (Yamada et al., 1994), although whether CES1A1 is the only enzyme responsible for the conversion of oseltamivir remains to be examined. MRP4 is also expressed on the luminal membranes of human brain capillaries (Nies et al., 2004; Bronger et al., 2005). Because oseltamivir crosses the BBB, Ro 64-0802 can be produced during the penetration of oseltamivir across the BBB and then be subjected to active efflux by MRP4. Although Northern blotting did detect OAT3 mRNA expression in the human brain (Cha et al., 2001), its distribution and membrane localization remain to be determined. Therefore, whether Ro 64-0802 can penetrate into the brain and is eliminated from the brain by OAT3 in humans, as well as in mice, also remains in question. Fluctuations in their activities will cause interindividual variations in their exposure to the central nervous system. For instance, genetic variations have been reported for P-gp and MRP4, which may alter their transport activities and expression. The silent mutation 3435C>T is associated with reduced P-gp expression (Hoffmeyer et al., 2000) and affects protein folding, resulting in a substrate-dependent functional change (Kimchi-Sarfaty et al., 2007). In MRP4, the nonsynonymous mutations 559G>T, 1460G>A, and 2269G>A are associated with altered transport activity and expression (Abla et al., 2008; Krishnamurthy et al., 2008). It is possible that these polymorphisms are associated with the adverse effects of Ro 64-0802 on the central nervous system.

In conclusion, Mrp4 and Oat3 are responsible for the elimination of Ro 64-0802 from the brain across the BBB although, at steady-state, Oat3 may not affect its brain distribution, probably because of its possible contribution also to the brain uptake of Ro 64-0802. This is the first demonstration of the cooperation of uptake and efflux transporters in the directional (brain-to-blood) transport of anionic drugs across the BBB.

**Acknowledgments.** We thank Dr. Junko Iida and Futoshi Kurotobi (Shimadzu) for technical support with the LC-MS system.

## References

Abla N, Chinn LW, Nakamura T, Liu L, Huang CC, Johns SJ, Kawamoto M, Stryke D, Taylor TR, Ferrin TE, Giacomini KM, and Kroetz DL (2008) The human multidrug resistance protein 4 (MRP4, *ABCC4*): functional analysis of a highly polymorphic gene. *J Pharmacol Exp Ther* 325:859–868.

Bakhiya A, Bahn A, Burckhardt G, and Wolff N (2003) Human organic anion transporter 3 (hOAT3) can operate as an exchanger and mediate secretory urate flux. *Cell Physiol Biochem* 13:249–256.

Bardsley-Elliot A and Noble S (1999) Oseltamivir. *Drugs* 58:851–860; discussion 861–862.

Belinsky MG, Guo P, Lee K, Zhou F, Kotova E, Grinberg A, Westphal H, Shchaveleva I, Klein-Szanto A, Gallo JM, et al. (2007) Multidrug resistance protein 4 protects bone marrow, thymus, spleen, and intestine from nucleotide analogue-induced damage. *Cancer Res* 67:262–268.

Bronger H, König J, Kopplow K, Steiner HH, Ahmadi R, Herold-Mende C, Keppler D, and Nies AT (2005) ABCC drug efflux pumps and organic anion uptake transporters in human gliomas and the blood-tumor barrier. *Cancer Res* 65:11419–11428.

Cha SH, Sekine T, Fukushima JI, Kanai Y, Kobayashi Y, Goya T, and Endou H (2001) Identification and characterization of human organic anion transporter 3 expressing predominantly in the kidney. *Mol Pharmacol* 59:1277–1286.

Ci L, Kusuhara H, Adachi M, Schuetz JD, Takeuchi K, and Sugiyama Y (2007) Involvement of MRP4 (ABCC4) in the luminal efflux of ceftizoxime and cefazolin in the kidney. *Mol Pharmacol* 71:1591–1597.

Deguchi T, Kusuhara H, Takadate A, Endou H, Otagiri M, and Sugiyama Y (2004) Characterization of uremic toxin transport by organic anion transporters in the kidney. *Kidney Int* 65:162–174.

Fuyuno I (2007) Tamiflu side effects come under scrutiny. *Nature* 446:358–359.

Hasegawa M, Kusuhara H, Adachi M, Schuetz JD, Takeuchi K, and Sugiyama Y (2007) Multidrug resistance-associated protein 4 is involved in the urinary excretion of hydrochlorothiazide and furosemide. *J Am Soc Nephrol* 18:37–45.

He G, Massarella J, and Ward P (1999) Clinical pharmacokinetics of the prodrug oseltamivir and its active metabolite Ro 64-0802. *Clin Pharmacokinet* 37:471–484.

Hill G, Cihlar T, Oo C, Ho ES, Prior K, Wiltshire H, Barrett J, Liu B, and Ward P (2002) The anti-influenza drug oseltamivir exhibits low potential to induce pharmacokinetic drug interactions via renal secretion-correlation of in vivo and in vitro studies. *Drug Metab Dispos* 30:13–19.

Hoffmeyer S, Burk O, von Richter O, Arnold HP, Brockmöller J, Johne A, Cascorbi I, Gerloff T, Roots I, Eichelbaum M, et al. (2000) Functional polymorphisms of the human multidrug-resistance gene: multiple sequence variations and correlation of one allele with P-glycoprotein expression and activity in vivo. *Proc Natl Acad Sci U S A* 97:3473–3478.

Imaoka T, Kusuhara H, Adachi M, Schuetz JD, Takeuchi K, and Sugiyama Y (2007) Functional involvement of multidrug resistance-associated protein 4 (MRP4/ABCC4) in the renal elimination of the antiviral drugs adefovir and tenofovir. *Mol Pharmacol* 71:619–627.

Izumi Y, Tokuda K, O'dell KA, Zorumski CF, and Narahashi T (2007) Neuroexcitatory actions of Tamiflu and its carboxylate metabolite. *Neurosci Lett* 426:54–58.

Kakee A, Terasaki T, and Sugiyama Y (1996) Brain efflux index as a novel method of analyzing efflux transport at the blood-brain barrier. *J Pharmacol Exp Ther* 277:1550–1559.

Kikuchi R, Kusuhara H, Abe T, Endou H, and Sugiyama Y (2004) Involvement of multiple transporters in the efflux of 3-hydroxy-3-methylglutaryl-CoA reductase inhibitors across the blood-brain barrier. *J Pharmacol Exp Ther* 311:1147–1153.

Kikuchi R, Kusuhara H, Sugiyama D, and Sugiyama Y (2003) Contribution of organic anion transporter 3 (Slc22a8) to the elimination of p-aminohippuric acid and benzylpenicillin across the blood-brain barrier. *J Pharmacol Exp Ther* 306:51–58.

Kimchi-Sarfaty C, Oh JM, Kim IW, Sauna ZE, Calcagno AM, Ambudkar SV, and Gottesman MM (2007) A "silent" polymorphism in the MDR1 gene changes substrate specificity. *Science* 315:525–528.

Krishnamurthy P, Schwab M, Takenaka K, Nachagari D, Morgan J, Leslie M, Du W, Boyd K, Cheok M, Nakauchi H, et al. (2008) Transporter-mediated protection against thiopurine-induced hematopoietic toxicity. *Cancer Res* 68:4983–4989.

Leggas M, Adachi M, Scheffer GL, Sun D, Wielinga P, Du G, Mercer KE, Zhuang Y, Panetta JC, Johnston B, et al. (2004) Mrp4 confers resistance to topotecan and protects the brain from chemotherapy. *Mol Cell Biol* 24:7612–7621.

Lindegardh N, Davies GR, Tran TH, Farrar J, Singhasivanon P, Day NP, and White NJ (2006) Rapid degradation of oseltamivir phosphate in clinical samples by plasma esterases. *Antimicrob Agents Chemother* 50:3197–3199.

Lowry OH, Rosebrough NJ, Farr AL, and Randall RJ (1951) Protein measurement with Folin phenol reagent. *J Biol Chem* 193:265–267.

Mori M, Hosokawa M, Ogasawara Y, Tsukada E, and Chiba K (1999) cDNA cloning, characterization and stable expression of novel human brain carboxylesterase. *FEBS Lett* 458:17–22.

Mori S, Ohtsuki S, Takanaga H, Kikkawa T, Kang YS, and Terasaki T (2004) Organic anion transporter 3 is involved in the brain-to-blood efflux transport of thiopurine nucleobase analogs. *J Neurochem* 90:931–941.

Mori S, Takanaga H, Ohtsuki S, Deguchi T, Kang YS, Hosoya K, and Terasaki T (2003) Rat organic anion transporter 3 (rOAT3) is responsible for brain-to-blood efflux of homovanillic acid at the abluminal membrane of brain capillary endothelial cells. *J Cereb Blood Flow Metab* 23:432–440.

Morimoto K, Nakakariya M, Shirasaka Y, Kakinuma C, Fujita T, Tamai I, and Ogihara T (2008) Oseltamivir (Tamiflu) efflux transport at the blood-brain barrier via P-glycoprotein. *Drug Metab Dispos* 36:6–9.

Nies AT, Jedlitschky G, König J, Herold-Mende C, Steiner HH, Schmitt HP, and Keppler D (2004) Expression and immunolocalization of the multidrug resistance proteins, MRP1–MRP6 (ABCC1–ABCC6), in human brain. *Neuroscience* 129:349–360.

Nozaki Y, Kusuhara H, Kondo T, Iwaki M, Shiroyanagi Y, Nakayama H, Horita S, Nakazawa H, Okano T, and Sugiyama Y (2007) Species difference in the inhibitory effect of nonsteroidal anti-inflammatory drugs on the uptake of methotrexate by human kidney slices. *J Pharmacol Exp Ther* 322:1162–1170.

Ohtsuki S, Asaba H, Takanaga H, Deguchi T, Hosoya K, Otagiri M, and Terasaki T (2002) Role of blood-brain barrier organic anion transporter 3 (OAT3) in the efflux of indoxyl sulfate, a uremic toxin: its involvement in neurotransmitter metabolite clearance from the brain. *J Neurochem* 83:57–66.

Ose A, Kusuhara H, Yamatsugu K, Kanai M, Shibasaki M, Fujita T, Yamamoto A, and Sugiyama Y (2008) P-glycoprotein restricts the penetration of oseltamivir across the blood-brain barrier. *Drug Metab Dispos* 36:427–434.

Reid G, Wielinga P, Zelcer N, van der Heijden I, Kuil A, de Haas M, Wijnholds J, and Borst P (2003) The human multidrug resistance protein MRP4 functions as a prostaglandin efflux transporter and is inhibited by nonsteroidal antiinflammatory drugs. *Proc Natl Acad Sci U S A* 100:9244–9249.

Roberts LM, Black DS, Raman C, Woodford K, Zhou M, Haggerty JE, Yan AT, Cwirla SE, and Grindstaff KK (2008) Subcellular localization of transporters along the rat blood-brain barrier and blood-cerebral-spinal fluid barrier by in vivo biotinylation. *Neuroscience* 155:423–438.

Satoh K, Nonaka R, Ogata A, Nakae D, and Uehara S (2007) Effects of oseltamivir phosphate (Tamiflu) and its metabolite (GS4071) on monoamine neurotransmission in the rat brain. *Biol Pharm Bull* 30:1816–1818.

Shi D, Yang J, Yang D, LeCluyse EL, Black C, You L, Akhlaghi F, and Yan B (2006) Anti-influenza prodrug oseltamivir is activated by carboxylesterase human carboxylesterase 1, and the activation is inhibited by antiplatelet agent clopidogrel. *J Pharmacol Exp Ther* 319:1477–1484.

Usami A, Sasaki T, Satoh N, Akiba T, Yokoshima S, Fukuyama T, Yamatsugu K, Kanai M, Shibasaki M, Matsuki N, et al. (2008) Oseltamivir enhances hippocampal network synchronization. *J Pharmacol Sci* 106:659–662.

Wiltshire H, Wiltshire B, Citron A, Clarke T, Serpe C, Gray D, and Herron W (2000) Development of a high-performance liquid chromatographic-mass spectrometric assay for the specific and sensitive quantification of Ro 64-0802, an anti-influenza drug, and its pro-drug, oseltamivir, in human and animal plasma and urine. *J Chromatogr B Biomed Sci Appl* 745:373–388.

Yamada T, Hosokawa M, Satoh T, Moroo I, Takahashi M, Akatsu H, and Yamamoto T (1994) Immunohistochemistry with an antibody to human liver carboxylesterase in human brain tissues. *Brain Res* 658:163–167.

Yamaoka K, Tanigawara Y, Nakagawa T, and Uno T (1981) A pharmacokinetic analysis program (multi) for microcomputer. *J Pharmacobiodyn* 4:879–885.

Yamatsugu K, Kamijo S, Suto Y, Kanai M, and Shibasaki M (2007) A concise synthesis of Tamiflu: third generation route via the Diels-Alder reaction and the Curtius rearrangement. *Tetrahedron Lett* 48:1403–1406.

Yoshino T, Nisijima K, Shioda K, Yui K, and Kato S (2008) Oseltamivir (Tamiflu) increases dopamine levels in the rat medial prefrontal cortex. *Neurosci Lett* 438:67–69.

**Address correspondence to:** Dr. Yuichi Sugiyama, Department of Molecular Pharmacokinetics, Graduate School of Pharmaceutical Sciences, The University of Tokyo, 7-3-1 Hongo, Bunkyo-ku, Tokyo 113-0033, Japan. E-mail: sugiyama@mol.f.u-tokyo.ac.jp

BIOCHEMICAL PHARMACOLOGY 77 (2009) 238–247

available at www.sciencedirect.com

ScienceDirect

journal homepage: www.elsevier.com/locate/biochempharm

# Human carboxylesterases HCE1 and HCE2: Ontogenic expression, inter-individual variability and differential hydrolysis of oseltamivir, aspirin, deltamethrin and permethrin☆

*Dongfang Yang*[a], *Robin E. Pearce*[b], *Xiliang Wang*[a], *Roger Gaedigk*[b], *Yu-Jui Yvonne Wan*[c], *Bingfang Yan*[a,*]

[a] *Department of Biomedical and Pharmaceutical Sciences, Center for Pharmacogenomics and Molecular Therapy, University of Rhode Island Kingston, Kingston, RI 02881, United States*

[b] *Section of Developmental Pharmacology and Experimental Therapeutics, Division of Pediatric Pharmacology and Medical Toxicology, Children's Mercy Hospital and Clinics, 2401 Gillham Road, Kansas City, MO 64108, United States*

[c] *Department of Pharmacology, Toxicology and Therapeutics, University of Kansas Medical Center, Kansas City, KS 66160, United States*

ARTICLE INFO

*Article history:*
Received 7 September 2008
Accepted 6 October 2008

ABSTRACT

Carboxylesterases hydrolyze chemicals containing such functional groups as a carboxylic acid ester, amide and thioester. The liver contains the highest carboxylesterase activity and expresses two major carboxylesterases: HCE1 and HCE2. In this study, we analyzed 104 individual liver samples for the expression patterns of both carboxylesterases. These samples were divided into three age groups: adults (≥ 18 years of age), children (0 days–10 years) and fetuses (82–224 gestation days). In general, the adult group expressed significantly higher HCE1 and HCE2 than the child group, which expressed significantly higher than the fetal group. The age-related expression was confirmed by RT-qPCR and Western immunoblotting. To determine whether the expression patterns reflected the hydrolytic activity, liver microsomes were pooled from each group and tested for the hydrolysis of drugs such as oseltamivir and insecticides such as deltamethrin. Consistent with the expression patterns, adult microsomes were ~4 times as active as child microsomes and 10 times as active as fetal microsomes in hydrolyzing these chemicals. Within the same age group, particularly in the fetal and child groups, a large inter-individual variability was detected in mRNA (430-fold), protein (100-fold) and hydrolytic activity (127-fold). Carboxylesterases are recognized to play critical roles in drug metabolism and insecticide detoxication. The findings on the large variability among different age groups or even within the same age group have important pharmacological and toxicological implications, particularly in relation to pharmacokinetic alterations of ester drugs in children and vulnerability of fetuses and children to pyrethroid insecticides.



☆ This work was supported by NIH grants R01ES07965 and R01GM61988 (BY) and R01CA053596 (YJW).

* *Corresponding author.* Tel.: +1 401 874 5032; fax: +1 401 874-5048.
E-mail address: byan@uri.edu (B. Yan).

*Abbreviations:* GAPDH, glyceradehyde-3-phosphate dehydrogenase; HCE, human carboxylesterase; HPLC, high-performance liquid chromatography; PBS, phosphate buffered saline; RT-qPCR, reverse transcription-quantitative polymerase chain reaction.

0006-2952/$ – see front matter © 2008 Elsevier Inc. All rights reserved.
doi:10.1016/j.bcp.2008.10.005

## 1. Introduction

Carboxylesterases constitute a class of enzymes that hydrolyze chemicals containing such functional groups as a carboxylic acid ester, amide and thioester [1]. These enzymes are known to play important roles in drug metabolism and insecticide detoxication. Two major human carboxylesterases (HCE1 and HCE2) are abundantly expressed in the liver, whereas HCE2 is predominately expressed in the gastrointestinal tract [1,2]. In addition to the difference in tissue distribution, these two enzymes differ markedly in the hydrolysis of certain drugs. For example, HCE1, but not HCE2, rapidly hydrolyzes the anti-influenza viral agent oseltamivir [3,4]. In contrast, HCE2, but not HCE1, rapidly hydrolyzes the anticancer agent irinotecan [5]. In addition to hydrolyzing numerous compounds, carboxylesterases catalyze transesterification. In the presence of ethyl alcohol, HCE1 effectively converts the anti-platelet agent clopidogrel (a methyl ester) into ethyl clopidogrel [4].

The expression of carboxylesterase is altered by xenobiotics and pathological conditions. In human primary hepatocytes, therapeutic agents such as dexamethasone and phenobarbital cause a slight or moderate induction of HCE1 and HCE2 [6]. Dexamethasone and phenobarbital also alter the expression of rat carboxylesterases [7]. However, the pattern of the alteration is different. Phenobarbital moderately induces rat carboxylesterases (hydrolase A and hydrolase B), whereas dexamethasone profoundly suppresses the expression of these enzymes [7]. Suppression also occurs in human primary hepatocytes treated with the pro-inflammatory cytokine interleukin-6 (IL-6), and the suppression is achieved by transcriptional repression [8]. More importantly, the IL-6 mediated suppression strongly alters cellular responsiveness to therapeutic agents such as clopidogrel, irinotecan, and oseltamivir [8]. Hydrolysis of clopidogrel represents inactivation. In contrast, hydrolysis of irinotecan and oseltamivir leads to the formation of therapeutically active metabolites thus represents activation [5,9].

The expression of carboxylesterases is regulated in a developmental manner, and it seems likely that these enzymes are developmentally regulated in humans as well. One to two week old rats express no hydrolase A or B based on immunoblotting analysis [7]. Consistent with the low level expression of carboxylesterases, the intrinsic clearance of the pyrethroid deltamethrin through hydrolysis in 10-day-old rats is only ~3% of adult rats [10]. Even in 4-week-old rats, the intrinsic clearance is less than half of that of adult rats [10]. In addition, young animals are generally much more sensitive to pesticides such as organophosphates and pyrethroids [11–13]. Carboxylesterases are known to protect against these chemicals by hydrolysis in the case of pyrethroids or scavenging mechanism in the case of organophoaphates. The developmental regulation of human carboxylesterases remains to be established. A previous report by Pope et. al. [14] observed that infants differ from adults in the expression and hydrolytic activity of carboxylesterases, but the difference was statistically insignificant [14]. The Pope's study, however, used a small number of samples and had only five samples for each group.

In the current study, we analyzed a total of 104 individual liver samples for the expression patterns of HCE1 and HCE2. These samples were grouped according to age: adults (>18 years old), children (0–10) and fetuses. Multiple experimental approaches were used including RT-qPCR, Western analysis and enzymatic assays. The fetuses expressed lower carboxylesterases than the children, and the children expressed lower carboxylesterases than the adults. Overall, the expression of both HCE1 and HCE2 showed a large inter-individual variability with the largest variability in the fetal group.

## 2. Materials and methods

### 2.1. Chemicals and supplies

Acetaminophen, aspirin, naproxen, and salicylic acid were purchased from Sigma (St. Louis, MO). Clopidogrel and clopidogrel carboxylate were from ChemPacific (Baltimore, MD). Oseltamivir and oseltamivir carboxylate were from Toronto Research Chemicals (Canada). Deltamethrin and permethrin were purchased from ChemService (West Chester, PA). Deltamethrin had a purity of 99%, and permethrin was from a batch that contained a mixture of cis- and trans-isomers at a ratio of 46% and 52%, respectively. TaqMan probes were from Applied Biosystems (Foster City, CA). The antibody against glyceradehyde-3-phosphate dehydrogenase (GAPDH) was from Abcam (Cambridge, MA). Unless otherwise specified, all other reagents were purchased from Fisher Scientific (Pittsburgh, PA).

### 2.2. Liver RNA and microsomal samples

A total of 104 RNA samples were used in this study and some of the RNA samples were matched with microsomes. Pure RNA samples were purchased from (ADMET Technologies (Durham, NC). Liver tissues were acquired from the National Disease Research Interchange (Philadelphia, PA), the Midwest Transplant Network (Westwood, KS), the University of Maryland Brain and Tissue Bank for Developmental Disorders (Baltimore, MD), and the University of Washington Central Laboratory for Human Embryology (Seattle, WA). Isolation of total RNA from the liver tissues was described previously [15,16], and the quality was determined on an Experion RNA StdSens micro fluidic chip (Bio-Rad, Hercules, CA) or by electrophoresis. Microsomes of child and fetal livers were prepared by differential centrifugation as described previously [17]. Adult liver microsomes (individual samples) were from CellzDirect (Pittsboro, NC) and described previously [4]. The demographics of the RNA samples in each group are summarized in Table 1. The use of the human samples was approved by the Institutional Review Board.

Table 1 – Demographic data for RNA samples.

| Group | n | M/F | CA | AA | H | Others | Unk |
|---|---|---|---|---|---|---|---|
| Fetus | 48 | 26/22 | 19 | 17 | 1 | 5 | 6 |
| Child | 34 | 15/19 | 21 | 8 | 3 | 2 | |
| Adult | 22 | 14/8 | 19 | 2 | | | |

Abbreviations: M/F: male/female; CA: Caucasian-American; AA: African American; H: Hispanic; Unk: unknown.

### 2.3. Reverse transcription-quantitative polymerase chain reaction (RT-qPCR)

Total RNA (0.1 μg) was subjected to the synthesis of the first strand cDNA in a total volume of 25 μl with random primers and M-MLV reverse transcriptase. The reactions were conducted at 25 °C for 10 min, 42 °C for 50 min and 70 °C for 10 min. The cDNAs were then diluted 6-fold and quantitative PCR was performed with TaqMan Gene Expression Assay (Applied Biosystems, Foster City, CA). The TaqMan assay identification numbers were: HCE1, Hs00275607_m1 (NM_001266); HCE2, Hs00187279_m1 (NM_198061); and polymerase (RNA) II, Hs01108291_m1 (NM_000937). It should be noted that the HCE1 probe could detect both HCE1A1 and HCE1A2 transcripts. The PCR amplification was conducted in a total volume of 20 μl containing universal PCR master mixture (10 μl), gene-specific TaqMan assay mixture (1 μl), and cDNA template (3 μl). The cycling profile was 50 °C for 2 min, 95 °C for 10 min, followed by 40 cycles of 15 s at 95 °C and 1 min at 60 °C, as recommended by the manufacturer. Amplification and quantification were done with the Applied Biosystems 7900HT Real-Time PCR System. All samples were analyzed in triplicate and the signals were normalized to polymerase (RNA) II [18] and then expressed as relative levels of mRNA among all samples.

### 2.4. Western analysis

Microsomal proteins (1.5 μg) were resolved by 7.5% SDS-PAGE in a mini-gel apparatus and transferred electrophoretically to nitrocellulose membranes. After non-specific binding sites were blocked with 5% non-fat milk, the blots were incubated with an antibody against HCE1, HCE2 and GAPDH, respectively. The preparation of the antibodies against HCE1 and HCE2 was described elsewhere [6]. The primary antibodies were subsequently localized with goat anti-rabbit IgG conjugated with horseradish peroxidase, and horseradish peroxidase activity was detected with a chemiluminescent kit (SuperSignal West Pico). The chemiluminescent signals were captured by a KODAK Image Station 2000 and the relative intensities were quantified by the KODAK 1D Image Analysis Software.

### 2.5. Enzymatic assays

All enzymatic assays were carried out at 37 °C in a total volume of 100 μl. Pilot studies were performed to determine conditions (e.g., protein concentrations) to maintain the metabolism in the linear range. Generally, microsomes (20–80 μg protein) were prepared in 50 μl incubation buffer (phosphate buffer, 100 mM, pH 7.4; or Tris–HCl, 50 mM, pH 7.4) and then mixed with an equal volume of substrate solution (the same buffer). Hydrolysis of aspirin was performed in phosphate buffer, whereas hydrolysis of oseltamivir, deltamethrin and permethrin was carried out in Tris–HCl buffer. Aspirin was assayed at 1 mM, oseltamivir at 200 μM, both deltamethrin and permethrin at 100 μM. The incubations lasted for 10–60 min depending on a substrate, and the reactions were terminated with 150 μl of acetonitrile containing an internal standard (IS): acetaminophen (750 ng/ml) for aspirin, clopidogrel carboxylate (50 ng/ml) for oseltamivir, napronex (4 μg/ml) for deltamethrin and clopidogrel (33 μg/ml) for permethrin. The reaction mixtures were subjected to centrifugation for 15 min at 4 °C (15,000 *g*). Hydrolysis of aspirin and oseltamivir was previously reported [3,4]. It should be noted that various controls were performed such as 0 min incubation and incubation without microsomes.

### 2.6. Monitoring of hydrolysis by HPLC or LC–MS/MS

The hydrolysis of aspirin or pyrethroids was separated by high-performance liquid chromatography (HPLC) (Hitachi LaChrom Elite-300) with a Chromolith SpeedROD column RP-18e (Merck, Germany). The supernatants (10–30 μl) of the reaction mixtures were injected and separated by an isocratic for aspirin or gradient mobile phase for deltamethrin and permethrin. The isocratic mobile phase consisted of 12% methanol and 0.25% acetate acid at pH 3.9 [4]. The gradient mobile phase consisted of acetonitrile and 0.01% formic acid. The gradient was run at 20–50% acetonitrile (v/v) for 6 min, 50–80% for 3 min followed by 80–20% for 6 min. Both mobile phases were run at a flow rate of 2 ml/min. For aspirin, the formation of hydrolytic metabolite was monitored, whereas for deltamethrin and permethrin the disappearance of parent compounds was monitored by a diode array detector at 230 nm. All quantifications were performed using peak area ratios and calibration curves generated from the internal control. The calibration curve ranged from 2 to 300 μg/mL with good linearity for salicylic acid, 0.8–160 μg/mL for deltamethrin, and 0.6–120 μg/mL for permethrin.

The hydrolysis of oseltamivir was monitored by LC–MS/MS system (API 3200) as described previously [3]. Briefly, the supernatants of the incubation mixtures were separated isocratically using a mobile phase composition of 70:30% (v/v) acetonitrile: 0.05% (v/v) formic acid in deionized water maintained at a flow rate of 0.25 ml/min with a total run time of 6.0 min. Detection of the analytes was performed in positive ion mode using the mass transitions of *m/z*: 313.3 → 166.1 for oseltamivir, *m/z*: 285.2 → 138.0 for oseltamivir carboxylate and *m/z*: 308.2 → 152.0 for IS. Flow injection analysis was performed at a flow rate of 20 μl/min to obtain optimum source parameters. The following compound parameters were used for oseltamivir, oseltamivir carboxylate and IS, respectively. Declustering potential: +5, +5 and +30 V, focusing potential: +360 V each, entrance potential: +8 V each, collision cell entrance potential: +20 V each, collision energy: +25, +25 and +30 V and collision cell exit potential: +7 V each. The optimum source parameters that gave the highest oseltamivir intensity were Curtain gas: 10 psi, collision gas: 4 psi, ion spray voltage: +5500 V, temperature: 450 °C, ion source gas1: 25 psi and ion source gas2: 85 psi. Integration of the peaks was performed by manual baseline adjustment using the ANALYST SP version 1.2 software (Applied Biosystems). All quantifications were performed using peak area ratios and calibration curves consisted of oseltamivir or oseltamivir carboxylate to clopidogrel carboxylic acid concentration ratios plotted against the oseltamivir or oseltamivir carboxylate to clopidogrel carboxylic acid peak area ratios. The calibration curve ranged from 1 to 250 ng/mL with good linearity for oseltamivir and 4 to 1000 ng/mL for oseltamivir carboxylate.